Analysis of the Temporal Behavior of Coherent Scatterers (CSs) in ALOS PalSAR Data

L. Marotti, R. Zandona-Schneider & K.P. Papathanassiou

German Aerospace Center (DLR)
Microwaves and Radar Institute0
PO.BOX 11 16, D-82230 Weßling, Germany
Email: luca.marotti@dlr.de

Abstract - **Coherent Scatterers (CSs) are scatterers detected by using spectral correlation properties and characterized by a deterministic scattering behavior. In this paper we investigate, for the first time, the temporal behavior of CSs using quad-pol data acquired by ALOS/PalSAR. In this sense, we can evaluate the stability of the deterministic scattering nature of individual scatterers.**

Keywords: Coherent Scatterers, Temporal behaviour, ALOS PALSAR.

I. INTRODUCTION

Coherent Scatterers (CSs) are scatterers characterized by a deterministic point-like scattering behavior. The detection of CSs can be performed even on the basis of a single SAR image, by exploiting spectral correlation properties addressed in terms of image sub-look (spectral) correlation [1]. The (amount of) spectral correlation of a scatterer is linked with its nature: highly coherent CSs represent very much point-like scatterers with almost deterministic scattering behavior while less coherent CSs are primarily scatterers with a developed speckle pattern and therefore with a stochastic scattering behavior. CSs with intermediate spectral coherence correspond to scatterers characterized by an intermediate speckle pattern development stage.

The launch of JAXA's ALOS in January 2006 provides for the first time the opportunity to acquire time series of polarimetric data from space. Indeed, PalSAR (i.e. the SAR instrument onboard of ALOS) is able to operate in a quad-pol mode - declared by JAXA as an "Experimental Mode" - that allows the acquisition of polarimetric data at L-band. This allows the investigation of the temporal behavior of CSs and to monitor changes in the coherent/incoherent nature of scatterers.

At this point it is important to discuss the difference between CSs and another category of important "coherent" scatterers, the so called Permanent Scatterers (PSs): PSs are also point-like scatterers with a stable scattering characteristic over large time periods. Therefore [2], the stability (in time) refers to their scattering phase behavior and requires a scattering pattern that does not change in time. On the other hand, the temporal stability of CSs do not necessarily requires a stable scattering behavior as long as the deterministic nature of the CSs is not changing. In the following we investigate the temporal behavior of CSs using quad-pol data acquired by ALOS/PalSAR.

II. CSs DETECTION

In [1] two approaches have been described for the estimation of CSs, both based on sub-look spectral correlation of SAR images. The simpler one evaluates the correlation coefficient between two parts of the full image spectrum (two sub-looks) and associates the pixels with high sub-looks correlation values to coherent scatterers, because only point scatterers are expected to have high spectral correlation.

In urban or even natural environments, one expects that the larger the resolution cell is the lower is the probability to find a dominant scatterer within it. Therefore, for the efficiency of the procedure, a wide system bandwidth is of advantage, in order to avoid the search of CSs in too large resolution cells. However, the detection of CSs using the relative narrow bandwidth ALOS/PALSAR system (14MHz in the quad-pol mode) has been demonstrated [3].

For the detection of CSs, two parameters have to be fixed: the estimation window size and the applied threshold value. The choice of an optimal window size is an estimation problem. Larger window sizes have the advantage of a low estimation bias but reduce the spatial resolution of the detection. This is a serious disadvantage for the detection of point-like scatterers. On the other hand, smaller windows allow higher spatial estimation accuracy but are affected by a stronger estimation bias. However, the fact that the estimation bias is smaller at high correlation values legitimates the use of the advantageous small window sizes. In [1] the detection of CSs as a function of the threshold has been addressed. It has been shown that by increasing the correlation threshold, the number of detected CSs decreases but their point-like scattering characteristics increase. We concluded, that the used threshold is direct related to how similar the CS response to an ideal point scatterer response is.

The temporal behaviour of CSs has been analyzed using a set of six ALOS images acquired over the Munich test site in fully polarimetric mode and with a repeat pass time of 46 days (see Table I) covering a total time period of about 7.5 months.

TABLE I.   AVAILABLE ALOS/PALSAR SCENES

Scene ID	P. Type	P. Level	Acquisition Date
ALPSRP022952630	PLR	1.1	2006 06 30
ALPSRP029662630	PLR	1.1	2006 08 15
ALPSRP036372630	PLR	1.1	2006 09 30
ALPSRP043082630	PLR	1.1	2006 11 15
ALPSRP049792630	PLR	1.1	2006 12 31
ALPSRP056502630	PLR	1.1	2007 02 15

The detected CSs are shown in Fig 1. The different colours are related to CSs detected at different polarizations indicating the strong polarimetric behaviour of CSs. As expected the density of CSs is high in the urbanized regions (i.e. over the city of Munich in the lower third of the image) due to the presence of many man-made (deterministic) objects.
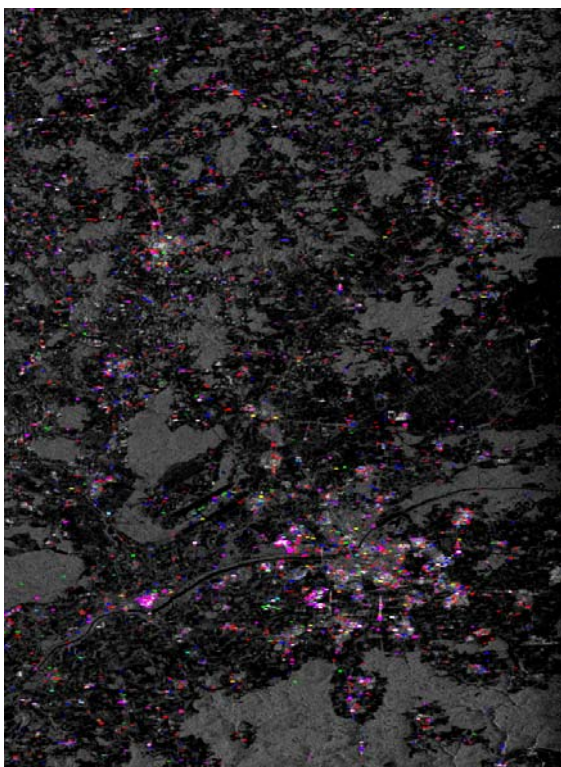

Figure 1.   Detected CSs in the Munich test site at different polarizations (Red: HH, Blue:VV, Green: HV)

In order to investigate the behaviour of the detected CSs in time, the detection procedure has been performed on each image and the number of common CSs has been evaluated. The obtained results are plotted in Figure 2. The green (continuous) lines represent the decay of the common CSs detected using four different threshold values. As expected, the number of CSs decreases monotonically with time demonstrating the temporal instability of many CSs. This can be due to different reasons: due to a change of the CS-to-background ratio, caused by a change of the background scattering behavior (the CS is not anymore the dominant scatterer within the resolution cell)
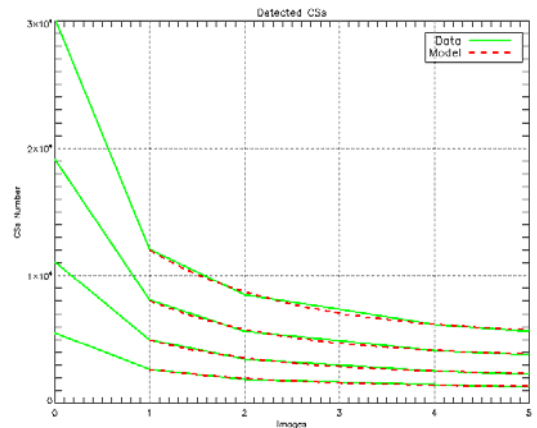

Figure 2.   Number of common CSs as a function of time (continuous green line) and prediction of the temporal decay model (dashed red line).

or simply because the CS is not anymore present in the resolution cell. However, as expected, a certain number of point-like scatterers is preserved from decorelation phenomena and remains stable in time.

III.   TEMPORAL MODEL

To describe the temporal behavior of the detected CSs an exponential decay model is assumed as:

$$N = S \, \exp(-a \, t) + L \qquad\qquad -1)$$

- N is the number of common detected CSs;
- S is the number of "short time" stable CSs;
- L is the number of "long time" stable CSs reached at convergence;
- a is the "attenuation" factor.

The model of Eq. 1 is fitted for the individual threshold values to the data and plotted (dashed) in red in Fig. 2. A good, in general, agreement with the experimental data is obtained that justifies the use of the model for comparison reasons.

In order to further evaluate the ability of the model to fit the data, the Root Mean Square Error Percentage (RMSEP) for a wider range of threshold values has been evaluated and plotted in Fig. 3. The error is always relatively small; the maximum of about 5% is reached for (coherence) threshold values around 0.55. However for higher threshold values, around 0.9, the error lies below 3%. It is necessary to note that those values of threshold are the more suitable for the detection of ideal point-like scatterers. The instability at higher threshold levels is due to the very low number of detected CSs.

In Fig. 4, the L/(L+S) ratio as a function of the estimation threshold is given. It is a measure for the quantity of finally reached stable CSs with respect to the potential stable CSs detected (i.e. CSs common between the first two images). Once more, it makes clear that high detection thresholds lead to the detection of more temporal stable CSs. Accordingly, higher
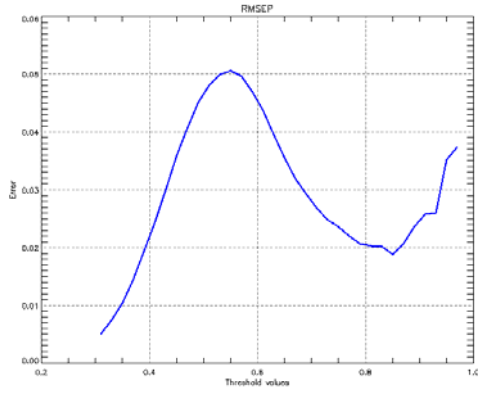
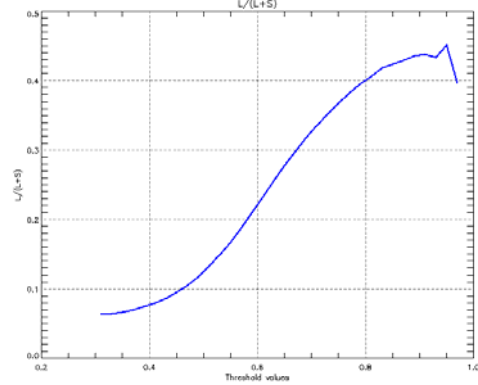Figure 3. RMSEP as a function of CS detection threshold.

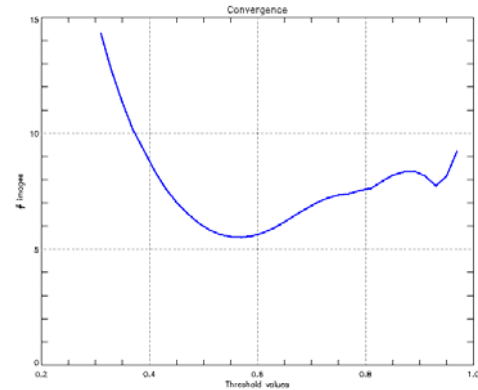Figure 4. L/(L+S) ratio as a function of CS detection threshold.

Figure 5. Temporal Convergence of CSs as a function of CSs detection threshold.

coherent points change their degree of sublook coherence slower than lower coherent CSs. Also here, the very low number of detected CSs at higher threshold levels caused some instability.

Let us now evaluate the time (# of images/acquisitions) necessary to reach L, i.e. the number of "long time" stable CSs. The model of Eq. 1 allows us to perform such estimation by increasing the time (t) until 0.5% of the convergence value (L) is reached. The values obtained in function of the estimation threshold are shown in Fig. 5. As we can see, even for low threshold values (around 0.4), the convergence is

reached within 15 acquisitions while at higher thresholds 7-8 acquisitions are enough.

TABLE II. CS TEMPORAL MODEL PARAMETERS

Threshold	a	L	S
0.60	-1.14	25e04	77e3
0.70	-0.85	7e04	36e3
0.80	-0.74	2e04	15e3
0.90	-0.68	4e03	3e3
0.97	-0.62	5e02	3e2

IV. POLARIMETRIC ANALYSIS

The scattering nature of a scattering process can be interpreted by evaluating its polarimetric signature. The detected CSs can be related to different canonical scattering mechanisms allowing a more qualitative understanding of their scattering behavior. In this sense, by using the α scattering angle

$$\alpha = \cos^{-1}\left(\frac{1}{\sqrt{2}} * \frac{|S_{HH} + S_{VV}|}{\sqrt{|S_{HH}|^2 + |S_{VV}|^2 + 4*|S_{HV}|^2}} \right) \qquad -2)$$

where S_{ij} are the elements of the scattering matrix it is possible to interpret CSs in terms of three canonical scattering categories:

- Surface scatterers $\qquad \alpha \leq 35°$
- Dipol scatterers $\qquad 35° \leq \alpha \leq 55°$
- Dihedrals scatterers $\qquad 55° \leq \alpha$

Accordingly, α has been evaluated for every detected CS and classified into one of the three categories. Figure 6 shows the normalized histogram of common CSs as a function of scattering angle α. It makes clear that the majority of the CSs are dihedrals while a still significant number is of dipole and surface type. For each category now the temporal evolution of the number of the common CSs has been performed. The results are similar to the ones obtained in Section III. This is one more indication for the suitability of the model to interpret the temporal behavior of CSs.
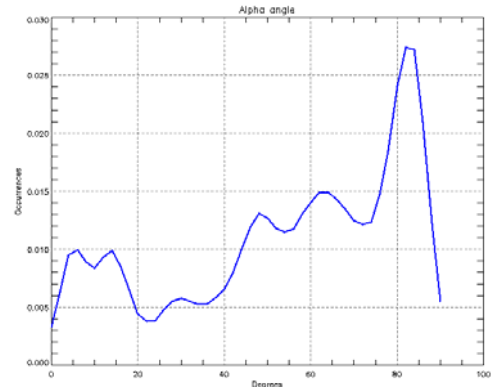

Figure 6. Normalised histogram of common CSs as a function of scattering angle α (i.e. scattering type).

In Fig. 7, the L/(L+S) ratio for the three scattering types is plotted. While for the surface and dipole scatterers the trend is very similar, the dihedral scatterers show a slightly different behavior at the higher thresholds: There, detected dihedral CSs have a higher probability to be stable in time. This is most probably linked with the high CS-to-background scattering amplitude ratio that characterizes highly coherent dihedral CSs.
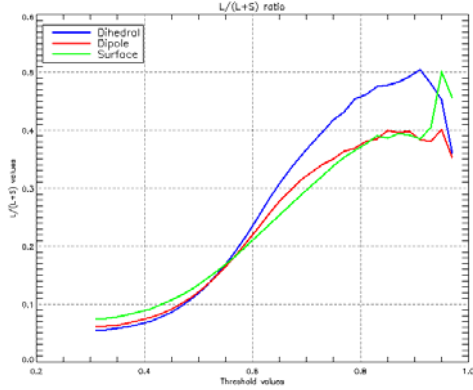

Figure 7. L/(L+S) ratio as a function of CS detection threshold for the different CSs types (Blue: Dihedrals, Red: Dipoles, Green: Surfaces).

V. FARADAY ROTATION

In the case of ALOS PalSAR the presence of an active ionospheric layer introduces an (additional) polarimetric distortion in form of a rotation of the polarization ellipse about an angle Ω as the wave propagates through (on transmit and receive), known as Faraday rotation distortion:

$$\begin{bmatrix} O_{HH} & O_{HV} \\ O_{VH} & O_{VV} \end{bmatrix} = \begin{bmatrix} \cos\Omega & \sin\Omega \\ -\sin\Omega & \cos\Omega \end{bmatrix} \begin{bmatrix} S_{HH} & S_{HV} \\ S_{VH} & S_{VV} \end{bmatrix} \begin{bmatrix} \cos\Omega & \sin\Omega \\ -\sin\Omega & \cos\Omega \end{bmatrix} \quad -3)$$

The one way Faraday rotation angle Ω depends on the geographic location, the acquisition geometry (incidence angle) and the ionospheric activity, thus it can change from acquisition to acquisition. This distortion leads to a biased estimation of the scattering alpha angle according to:

$$\alpha^F = a\cos^{-1}(\cos(\ \alpha\ )\cos(\ 2\Omega\ )) \quad -4)$$

where α is the underlying and α^F the distorted scattering alpha angle. Figure 8 shows α^F as a function of Ω for the whole range of α values (i.e. [0, π/2]). One can see that, according to Eq. 4, surface and dipole like scatterers are stronger affected than dihedrals. Isotropic dihedrals (α=90°) are invariant under Faraday distortion as $\cos(\alpha)$ =0. This can be also a reason for the higher temporal stability of the dihedral CSs.

In order to correct for the Faraday distortion Ω has to be estimated for each scene individually. One way to do this is by using the circular polarization basis:

$$\tan(4\Omega) = \frac{2\,\mathrm{Re}(<(O_{HH}+O_{VV})(O_{HH}-O_{VV})^*>)}{<|O_{HH}+O_{VV}|^2 - |O_{HV}+O_{VH}|^2>} \quad -5)$$
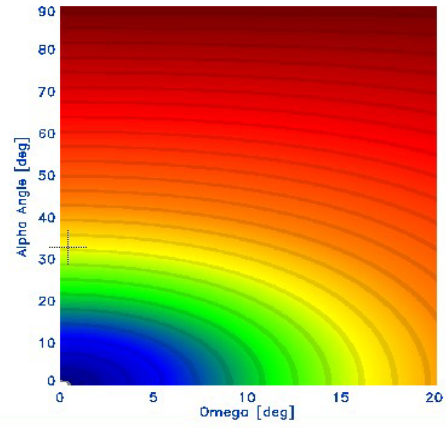
Figure 8. Scattering alpha angle α as a function of Faraday rotation angle Ω.

The estimated Faraday rotation angles Ω for each scene are listed in Table III.

TABLE III. ESTIMATED FARADAY ROTATION.

Scene ID	Acquisition Date	Ω [deg]
ALPSRP022952630	2006 06 30	1.2
ALPSRP029662630	2006 08 15	0.8
ALPSRP036372630	2006 09 30	3.4
ALPSRP043082630	2006 11 15	2.6
ALPSRP049792630	2006 12 31	1.7
ALPSRP056502630	2007 02 15	2.0

VI. CONCLUSIONS

In this paper the temporal behavior of CSs has been investigated using quad-pol data acquired by ALOS/PalSAR. An exponential model has been validated against the number of common detected CSs and used to extrapolate the temporal behavior of the stability of the deterministic scattering nature of individual CSs. Dihedral like CSs appear to be the majority of the detected CSs and appear more stable in time.

REFERENCES

[1] R.Z. Schneider, K.P. Papathanassiou, I. Hajnsek & A. Moreira, "Polarimetric and Interferometric Characterization of Coherent Scatterers in Urban Areas", *IEEE Trans. Geoscience and Remote Sensing*, vol. 44, No. 4, pp. 971-984, April 2006.

[2] A. Ferreti, C. Prati & F. Rocca, "Permanent scatterers in SAR interferometry," *IEEE Transactions on Geoscience and Remote Sensing*, vol. 39, no. 1, pp. 8-20, January 2001.

[3] L. Marotti, R.Z. Schneider & K.P. Papathanassiou, "Coherent Scatterers (CSs) Detection and Characterization with ALOS-PalSAR",. in *3rd Intl. Workshop on SAR Polarimetry and Polarimetric Interferometry (PolInSAR2007)*, Frascati, Italy, 22-26 January 2007.